

# Lawrence Berkeley National Laboratory

## Recent Work

### Title

TEE WOLTER PHASEPLATE IN ULTRACENTRIFUGATION AND ELECTROPHORESIS

### Permalink

<https://escholarship.org/uc/item/78q287th>

### Authors

Trautman, Rodes  
Burns, Victor W.

### Publication Date

1954

UCRL 2453  
UNCLASSIFIED

UNIVERSITY OF  
CALIFORNIA

*Radiation  
Laboratory*

TWO-WEEK LOAN COPY

*This is a Library Circulating Copy  
which may be borrowed for two weeks.  
For a personal retention copy, call  
Tech. Info. Division, Ext. 5545*

BERKELEY, CALIFORNIA

## **DISCLAIMER**

This document was prepared as an account of work sponsored by the United States Government. While this document is believed to contain correct information, neither the United States Government nor any agency thereof, nor the Regents of the University of California, nor any of their employees, makes any warranty, express or implied, or assumes any legal responsibility for the accuracy, completeness, or usefulness of any information, apparatus, product, or process disclosed, or represents that its use would not infringe privately owned rights. Reference herein to any specific commercial product, process, or service by its trade name, trademark, manufacturer, or otherwise, does not necessarily constitute or imply its endorsement, recommendation, or favoring by the United States Government or any agency thereof, or the Regents of the University of California. The views and opinions of authors expressed herein do not necessarily state or reflect those of the United States Government or any agency thereof or the Regents of the University of California.

UCRL-2453  
Unclassified - Instrumentation  
Distribution

**UNCLASSIFIED**

UNIVERSITY OF CALIFORNIA  
Radiation Laboratory  
Contract No. W-7405-eng-48

THE WOLTER PHASEPLATE  
IN ULTRACENTRIFUGATION AND ELECTROPHORESIS

Rodes Trautman and Victor W. Burns

January, 1954

Berkeley, California

THE WOLTER PHASEPLATE  
IN ULTRACENTRIFUGATION AND ELECTROPHORESIS

Rodes Trautman and Victor W. Burns

Donner Laboratory of Medical Physics and  
Radiation Laboratory, Department of Physics  
University of California, Berkeley, California

January, 1954

ABSTRACT

An inexpensive practical phaseplate available commercially is described. Illustrations are given of its use in electrophoresis and ultracentrifugation equipment as a schlieren diaphragm--the operational heart of the schlieren optical system. Practically, the use of the phaseplate is warranted when (a) high magnification angles are used, (b) the refractive index gradient curve is steep (c) disturbances in the cell are to be seen most clearly. Theoretically, the phaseplate confirms concepts of the nature of the diffraction fringes from any schlieren diaphragm, since it operates on diffraction due to defocusing of the light-source image by the lens action of the gradient. Distèche's and Wolter's theories of the fringes are contrasted. The phaseplate also makes more clear the nature of the anomaly of schlieren patterns near the baseline, which show different shapes according to the orientation of the opaque edge.

## THE WOLTER PHASEPLATE IN ULTRACENTRIFUGATION AND ELECTROPHORESIS

Rodes Trautman and Victor W. Burns

Donner Laboratory of Medical Physics and  
Radiation Laboratory, Department of Physics  
University of California, Berkeley, California

January, 1954

### Development of the Phaseplate

In 1950 Wolter<sup>1</sup> described a new type of schlieren diaphragm<sup>2</sup> which utilized Fresnel diffraction effects to yield on the photographic plate or ground glass of the schlieren camera a pattern having an intensity null at the true boundary position. In contrast to a diaphragm of opaque material with mechanical straight edges (such as a blade, bar, wire or slit), Wolter's completely transparent "phaseplate" employs an optical edge. The optical edge is the discontinuity at the edge of a uniform transparent coating over half of a supporting transparent glass plate. The coating is thus similar in size and position to the half plane or blade, except that it is transparent and of such a thickness that transmitted rays are one-half wavelength out of phase with adjacent rays not passing through the coating. The phaseplate edge can give a shadow on the ground glass only if the light-source image does not focus on it (i. e. does not focus in the plane of the schlieren diaphragm). Thus in principle straight baselines give no registration but peaks do, since boundary regions in a parallel-wall cell defocus the light-source image as well as deflect it<sup>3, 4</sup>. Each level in a boundary region can thus be represented by a prism accounting for the deflection and a lens accounting for the defocusing (schematically shown in Fig. 6). It is this defocused light-source image, illuminating the mechanical schlieren diaphragm, that casts the familiar Fresnel type diffraction pattern on the photographic plate<sup>5</sup>.

Various ways of obtaining the baseline and regions where there is no lens action (e. g. top of peak) are available when using a phaseplate.

(a) The edge of the phaseplate can be centered in a mechanical slit<sup>6, 7</sup>. The baseline is obtained by bisecting the slit pattern, which is well defined in those

regions in which the phaseplate pattern is missing.

(b) A very narrow wire (about  $1/4$  to  $1/3$  the diameter of a wire suitable for a diaphragm) gives the baseline regions but no peaks. Hence superposition of the wire accurately along the optical edge of the phaseplate gives both baseline and pattern of essentially the same width for all deflections. (An example of this appears later, Fig. 2a.

(c) The light source can be defocused; but this gives tilted baselines.

(d) If overexposure is avoided the very faint, extremely sharp line which does appear (owing probably to imperfections in the phaseplate) can be used.

Several methods of making a phaseplate were suggested by Wolter<sup>1</sup>. These were all tried unsuccessfully in this laboratory. Not until the American Optical Company, Instrument Division, Buffalo, N. Y., experts in phase coatings, were consulted was a usable phaseplate obtained. The coating is  $MgF_2$  evaporated onto the supporting plate, and is sufficiently durable that it can be cleaned with methanol and lens paper, and no cover glass is necessary. The cost of the coating is nominal; the price of the complete phaseplate is determined mainly by the cost of the supporting glass, chosen for (a) optical quality, (b) size, and (c) shape, including notches or holes for mounting purposes.

The purpose of this paper is to describe test experiments with the phaseplate and to present in greater detail the theory of its operation in a schlieren optical system.

#### Testing the Phaseplate

The tests of the phaseplates supplied by the American Optical Company for the mercury green line were made on both a Klett electrophoresis apparatus and a Spinco Model E ultracentrifuge.

The phaseplates were made from ordinary plate glass. Ideally, one would prefer an optical flat, but only a small region (approx. 1 mm) on either side of the edge is used, and repolished plate glass was found satisfactory. An unpolished plate glass with an observable "orange peel" surface gave good patterns except for the mottled background due directly to this "orange peel" surface (see Fig. 2a). (Figure 2a shows application of a wire 0.003 in. in diameter along the phaseplate edge to register baseline regions.

The plates were supplied round and notched so that they could be cemented to a brass ring to be attached to the diaphragm mount (see Fig. 1).

For the comparison pictures the brass ring carried also a wire (0.010 in. diameter) and a standard Spinco bar (1.5 mm).

The coating has a slight greenish tinge which has a negligible effect on transparency. It is essential that the edge be sharp, for if it is not, it acts as a cylinder lens and discriminates between the rays of the same deflection coming from the two sides of the boundary region. This causes a distortion of the pattern and is easily detected on a symmetrical gradient because the diffraction fringes inside the peak do not cross at the center. Contrast Fig. 2b, made with a poor phaseplate, with Fig. 3, made with a good quality phaseplate.

Figure 3a shows the appearance of a boundary in the ultracentrifuge with a wire (top), a phaseplate (center), and a bar (bottom). The three diaphragms were parallel and used simultaneously. The synthetic boundary cell<sup>8</sup> was used to get the boundary in the center of the cell. The double meniscus is due to a layer of mineral oil on the protein solution. Notice that with the phaseplate the baseline is almost invisible. Observe also that the diffraction fringes from the phaseplate have greater contrast than those of the wire or bar (a point to be discussed theoretically later). The fringes have essentially the same horizontal spacing for the three diaphragms at any chosen height above the baseline.

Figure 3b shows the same test on the Klett electrophoresis apparatus. Two exposures are shown. The phaseplate pattern remains sharp over a wide range of exposure, but loses the baseline on overexposure. This is in contrast to the wire pattern, which loses the peak while retaining the baseline. The bar pattern, on overexposure, reveals diffraction fringes inside, as pointed out previously by Kegeles<sup>9</sup>.

It has been the experience in this laboratory that the condition mentioned by Wolter on the size of the light-source slit is inapplicable, and all the pictures of this paper have been taken with conventional slit openings and exposure times. It has been observed, also (but not illustrated here by a photograph) that—as far as sharpness of detail is concerned—increasing the light-source slit width to as much as 0.5 mm is equivalent to increasing the exposure. Hence stringent restrictions on light-source slit width are not necessary in practice. Areas under the curves of Fig. 3a and 3b were measured and it was found that the



average of the bar patterns agreed with the wire and phaseplate patterns within the plate-reading error of  $\pm 1\%$ .

Figure 3c shows the boundary of Fig. 3a taken at very high magnification (small angle of the phaseplate as schlieren diaphragm). The wire or bar patterns would be unusable at this magnification. Thus the phaseplate retains its very narrow registration of the boundary (geometrical shadow) over the entire range of diaphragm angles. The phaseplate also retains its excellent registration for both steep- and shallow-gradient curves. This is in direct contrast to the wire pattern, which becomes poorer as the curve becomes steeper. The difference is shown in Fig. 4b, which is the sixth frame of a standard lipoprotein<sup>10</sup> run, using a single cell but using the wire (upper pattern) and the phaseplate (lower pattern) simultaneously for comparison purposes. Compare the patterns in the neighborhood of the vertical bar. Disturbances in the cell sometimes encountered in sedimenting as well as in floating runs are usually much more vividly portrayed by the phaseplate than by the wire or bar. An example is in Fig. 4a, where the upper pattern is the wire and the lower pattern is the phaseplate.

There is an outstanding anomaly of all schlieren diaphragms whereby the inside pattern appears with sharper "corners" than does the outside pattern at the tails of a bell-shaped peak. This is evident on the bar pattern of Figs. 3a and 3b, and can be seen also on blade (knife-edge) patterns if one reverses the blade so as to compare black on white and white on black patterns. The pattern in which the knife edge cuts out the undeflected light-source image as well as deflected rays (opaque upper half-plane in electrophoresis, for example) has sharper corners than the usual pattern in which the inside of the bell-shaped peak is a shadow region. With the phaseplate, since outside and inside patterns are merged to a single null-point registration, the nature of this anomaly becomes clear. It is due to the closer spacing of the diffraction fringes inside the pattern than outside. This is seen on all the pictures, but most vividly on Fig. 3c. The steeper the gradient, the greater this effect. Since the theory of the diffraction patterns, to be presented below, indicates only symmetrical diffraction patterns, this anomaly of the schlieren optical system poses a serious question whether in these regions there is accurate registration of the boundary. Thus, the averaging of inside and outside patterns with the bar, for example, takes care of size changes due to exposure variations, but does not take care of this difference

in shape of inside and outside patterns.

An attractive hypothesis for the explanation of the closer spacing of fringes inside the pattern is that the light rays equally deflected from the two sides of the boundary are somehow interacting to yield the diffraction pattern inside, but are effectively independent for the diffraction pattern outside. In Fig. 6, to be explained when the theory is considered, the light-source images at G and H from the two sides of the boundary would be considered as simultaneously casting an interfering Fresnel type diffraction pattern. As a test of this hypothesis a boundary was formed in the marco electrophoresis cell (7.5 mm channel width) so that the boundary region would be wide enough, left and right, to permit masking out, at the cell, light from each side of the boundary, leaving a vertical strip down the center of the cell that was not masked at all. If the hypothesis were correct, then the closer spacing in the center of the channel, inside the boundary, would now become greater and be equal to that outside the boundary left and right of the center where the masks were placed. Figure 5 shows the resulting photograph for one setting of the phaseplate in the electrophoresis apparatus. No cylindrical lens is used and the phaseplate is horizontal, representing one position in a scanning type pattern. It can be seen that the spacing inside the two sides of the boundary is closer than outside (which incidentally shows that the anomaly is not due to the cylindrical lens and diagonal diaphragm. But the spacing is not altered by the masks. Therefore the hypothesis is false. Hence, this phenomenon remains unexplained, and perhaps must wait for explanation until the schlieren optical system is treated completely by physical optics from the light source to the photographic plate, rather than by mixing geometrical and physical optics as indicated in the theory below.

#### Theory of the Fringes "Outside" the Shadow

There are two methods in the literature for deriving the expressions for the Fresnel fringes in the schlieren optical system. Both consider the schlieren camera without the cylindrical lens. The schlieren optical set up, however, even without the cylindrical lens, is still quite complex and in the usual arrangement the camera objective is between the diffracting edge (schlieren diaphragm) and the photographic plate. To avoid this complication Distèche<sup>11</sup> refers all

optical components to the neighborhood of the cell by geometrical optics, then treats the interaction of these elements by physical optics to get the intensity distribution in the plane in this neighborhood which by geometrical optics is imaged on the photographic plate. The details of the derivation are obscure, but the resulting fringe spacings are those of Fresnel diffraction from a knife edge. The absolute magnitude of the spacings in terms of the refractive index distribution and optical constants is  $\sqrt{2}$  times as large as the spacing predicted from Wolter's theory (if it is applied to the same diffracting element, a knife edge).

Wolter<sup>1</sup>, on the other hand, chooses an equivalent optical system which has no lenses between the schlieren diaphragm and the photographic plate. This is shown in Fig. 6. (Various equivalent optical systems are given by Svensson<sup>4</sup>). Geometrical optics are used to find the location of the light source after rays pass through the schlieren lens, the gradient lens, and the second schlieren lens acting also as a camera objective. This (defocused) light-source image is considered the source, the schlieren diaphragm the diffracting element, and the photographic plate the screen in the conventional Fresnel type diffraction problem. The method is only outlined by Wolter. Since it gives an insight into the schlieren optical system and allows derivation of fringe spacings (other than the anomaly mentioned earlier) for any type of diaphragm one may choose to use, the details are considered here. Because of the equivalence of the various schlieren optical systems the conclusions for the one of Fig. 6 are assumed valid in any system, including the diagonal-slit, cylindrical-lens set up.

First consider the lens action of the gradient. This has been described,<sup>3,4</sup> but a simple derivation will be given here. In Fig. 7 the cell is shown illuminated by two parallel rays. By definition, the focal length of the equivalent lens is the distance to the point of focus when illuminated by parallel light. From the drawing,  $-d\delta = dz/f$  where according to convention the upward direction of  $z$  is positive and focal length  $f$  is positive if the focal point is to the right of the cell. But the deflection of light passing through an index of refraction gradient is  $\delta = a \cdot dn/dz$  where  $a$  is the cell path length and  $n$  is the index of refraction of the solution in the cell at the location of the ray considered. Thus:

$$f = - \frac{dz}{d\delta} = - \frac{1}{a \frac{d^2 n}{dz^2}} = - \frac{1}{an} \quad (1)$$

The lens E of focal length  $b$  focuses the cell C on the plate P according to the lens formula

$$\frac{1}{m} + \frac{1}{n} = \frac{1}{b} \quad (2)$$

Its magnification  $M$  is expressible from (1) as

$$M = \frac{n}{m} = \frac{n - b}{b} \quad (3)$$

Rays through two portions of the boundary region are drawn in Fig. 6. The two regions are on either side of the maximum refractive-index gradient and have the same deflection. The effect of the gradient is schematically shown by the insert figures of a prism and a lens. The solvent side of the maximum gradient is concave (on a  $c$ -vs- $z$  plot), hence is a diverging lens, whereas the solution side is convex and is a converging lens. Just the converging side is considered. It focuses the light source at  $G'$ , which is now imaged by the lens E to point G by the lens formula

$$\frac{1}{m-f} + \frac{1}{g} = \frac{1}{b} \quad (4)$$

Solving this for  $b-g$ , the distance  $p$  of the source from the diffracting element, gives

$$p \equiv b - g = -\frac{b^2}{m - b - f} \quad (5)$$

The distance of the screen from the plate is

$$q \equiv n - b \quad (6)$$

Now in the Fresnel treatment a change of variable from the coordinate  $z$ , which is the distance on the plate from the geometrical shadow to the fringes, to  $v$  is desirable to make a universal plot, the Cornu Spiral, of the relationships involved. The transformation is

$$v = -z/k \quad (7)$$

where

$$k \equiv \sqrt{\frac{\lambda q (p + q)}{2p}}, \quad (8)$$

in which  $\lambda$  is the wavelength of light and  $p$  and  $q$  are the distances defined above. Note that in the schlieren case  $p$  is a function of position in the boundary region but  $q$  remains constant. When (5) and (6) are substituted for  $p$  and  $q$ , then  $k$  can be expressed in terms of  $m$ ,  $b$ , and  $f$ . Then from (1) and (3) it can be put in a more useful form:

$$k = \frac{n - b}{b} \sqrt{\frac{\lambda |f|}{2}} = M \sqrt{\lambda |f|/2} = M \sqrt{\lambda/(2a |n''|)} \quad (9)$$

(Absolute-value symbols have been used since the same numerical expression is valid for the diverging-boundary region yielding source H).

In Fig. 8 the actual phaseplate diaphragm D is considered. The supporting glass plate is not drawn. The source G corresponds to G of Fig. 6 and the point Q is the geometrical shadow of the optical edge A of the phaseplate. The Fresnel treatment<sup>12, 13</sup>, which is a special case of the more general Kirchoff treatment, states that the amplitude of the light at a point P on the plate can be obtained by integration of the wave contributions to P from differential elements along the wave front at D originating from G as source. It is assumed that the portions of D that contribute an appreciable amount to the amplitude at P are sufficiently close to the line  $\overline{GP}$  that the wave front can be assumed planar. When the Cornu Spiral, shown schematically for this problem in Fig. 9, is used, the  $v$ 's in the third quadrant are negative corresponding to distance  $s$  on the wave front below the origin 0 of the line  $\overline{GP}$ . From the geometry in Fig. 8 the relationship between  $s$  and  $z$  is

$$\frac{s}{z} = \frac{-p}{p+q} \quad (10)$$

so that the conversion of distance on a wave front  $s$  to the variable  $v$  can be determined (although not needed here) from (7), (8) and (10) as

$$v = \sqrt{\frac{2(p+q)}{pq\lambda}} \cdot s \quad (11)$$

The calculation of the amplitude at  $P_1$  will be considered. The distance  $z_1$  is negative, hence  $s_1$  and  $v_1$  are positive. All the contributions from D to the amplitude at  $P_1$  are (see Fig. 9):

$\overline{Z^1 0}$  : light passing through lower half plane between  $-\infty$  and  $0_1$

$\overline{0A}$  : light passing through lower half plane between  $0_1$  and A

$\overline{AZ}$  : light passing through upper half plane between A and  $+\infty$   
if no phase shift were involved.

$\overline{AZ^1} = \overline{A^1 Z^1}$  : correction of  $\overline{AZ}$  for the half-wave phase shift present in regions above A compared to regions below A.

$\overline{A^1 A}$  : net amplitude of light at  $P_1$  due to all light passing through phaseplate from  $-\infty$  to  $+\infty$

This result is generalized for any point P as follows: If  $E(v)$  is the amplitude of the vector from the origin of the spiral to the point v, where v corresponds to P, and  $E_p$  is the amplitude of the light vector at P, then

$$E_p = E(v) - E(-v) = 2E(v), \tag{12}$$

which is the relation given without derivation by Wolter<sup>1</sup>. The location of the maxima and minima of intensity can be found by determining which values of v maximize and minimize  $E(v)$ . It is usually considered that the  $45^\circ$  line cuts the spiral at the critical values  $v_c$ <sup>13</sup>. For maxima

$$v_c \Big|_{\max_i} = \sqrt{4i - 5/2} \quad i = 1, 2, 3, \dots \tag{13}$$

For minima

$$v_c \Big|_{\min_i} = \sqrt{4i - 1/2} \quad i = 1, 2, 3, \dots \tag{14}$$

and on the plate, using (7), (9) and (13) or (14), the location of the  $i^{\text{th}}$  fringe, counting the geometrical shadow null as zero, is:

$$z_c \Big|_{\min_0} = 0$$

$$z_c \Big|_{\min_i} = M \sqrt{\lambda / (2a |n''|)} \sqrt{4i - 1/2} \quad i = 1, 2, 3, \dots$$

$$z_c)_{\max_i} = M \sqrt{\lambda / (2a |n''|)} \sqrt{4i - 5/2} \quad i = 1, 2, 3 \dots$$

For the opaque upper half-plane as schlieren diaphragm the amplitude at  $P_1$ , using again Fig. 9, would be the amplitude of the vector  $\overline{Z'O} + \overline{OA} = \overline{Z'A}$ . The critical values of  $v$  for this vector as the head moves around the spiral are again very close to those cut by the  $45^\circ$  line and hence the spacing of the fringes with a mechanical edge will be the same as with a phaseplate, as observed qualitatively in the experimental section. The relative intensities between the first maximum and first minimum of the phaseplate pattern will be greater than with the knife edge. Thus

Knife edge:

$$\frac{I_{\max_1}}{I_{\min_1}} = \frac{1.34 I_0}{0.78 I_0} = 1.7$$

Phaseplate:

$$\frac{I_{\max_1}}{I_{\min_1}} = \frac{1.73 I_0}{0.59 I_0} = 2.9$$

Thus the phaseplate does not eliminate diffraction effects (in fact it intensifies the fringe pattern), but utilizes diffraction to give a null-point registration of true boundary positions.

This work was supported (in part) by the Atomic Energy Commission and by a grant from the Life Insurance Medical Research Fund.

References

1. H. Wolter, Ann. Physik 7, 182 (1950)
2. L. G. Longworth, Ind. and Eng. Chem. (Anal. Ed) 18, 219 (1946)
3. O. Lamm, Z. Physik. Chem. A 138, 313 (1928)
4. H. Svensson, Arkiv. Kemi, Mineral. Geol. 22A, No. 10 (1946)
5. L. G. Longworth, J. Am. Chem. Soc. 65, 1755 (1943)
6. W. Kossel and K. Strohmaier, Z. Naturforschg. 6a, 504 (1951)
7. O. Armbruster, W. Kossel and K. Strohmaier, Z. Naturforschg. 6a, 509 (1951).
8. E. G. Pickels, W. F. Harrington and H. K. Schachman, Proc. Nat. Acad. Sci. 38, 943 (1952)
9. G. Kegeles and F. Gutter, J. Am. Chem. Soc. 73, 3770 (1951)
10. J. W. Gofman et al., Science 111, 166 (1950)
11. A. Distèche Biochimica et Biophysica Acta 3, 146 (1949)
12. F. A. Jenkins and H. E. White, Fundamentals of Physical Optics, McGraw-Hill, 1937.
13. J. Volasek, Introductory Theoretical and Experimental Optics, John Wiley, 1949, p. 172-185.



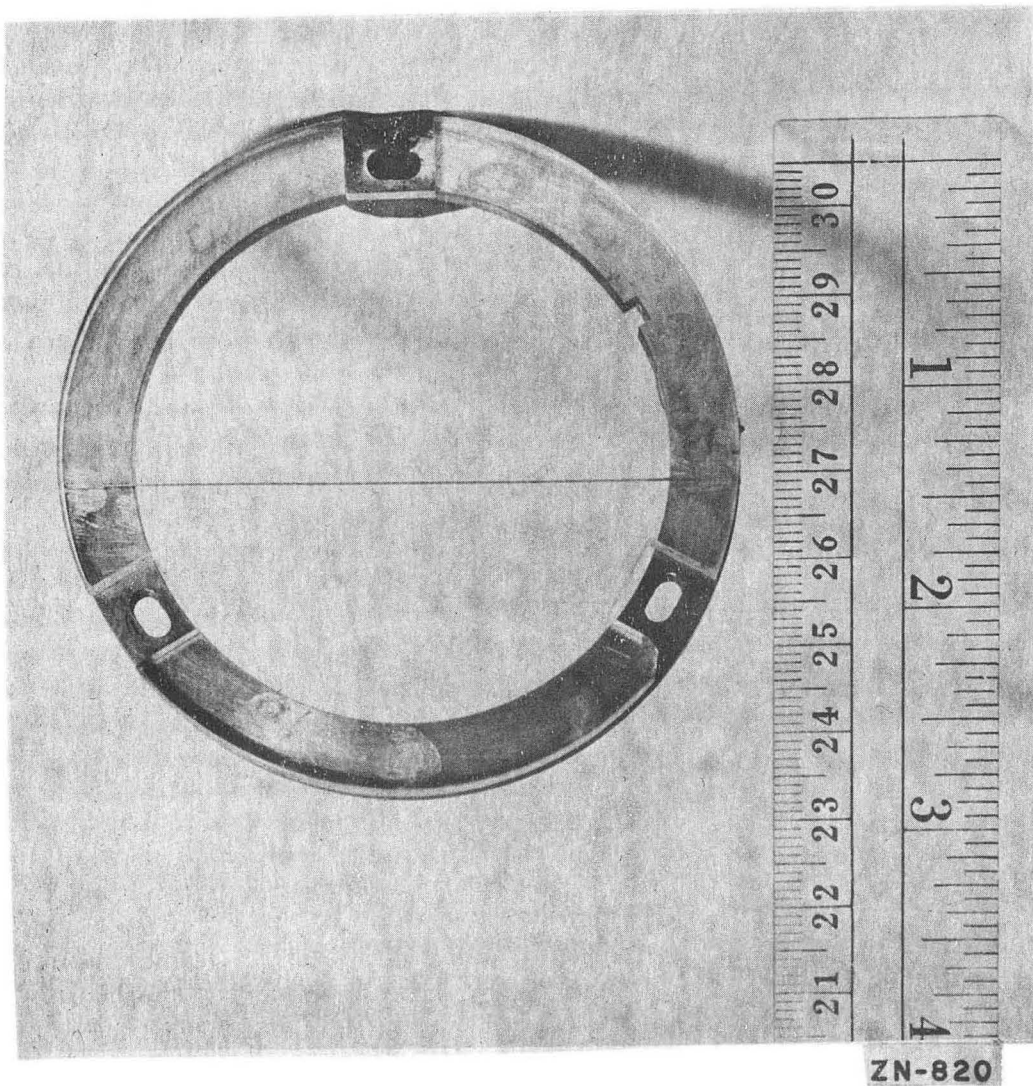


Fig. 1 - Phaseplate mounted on brass ring

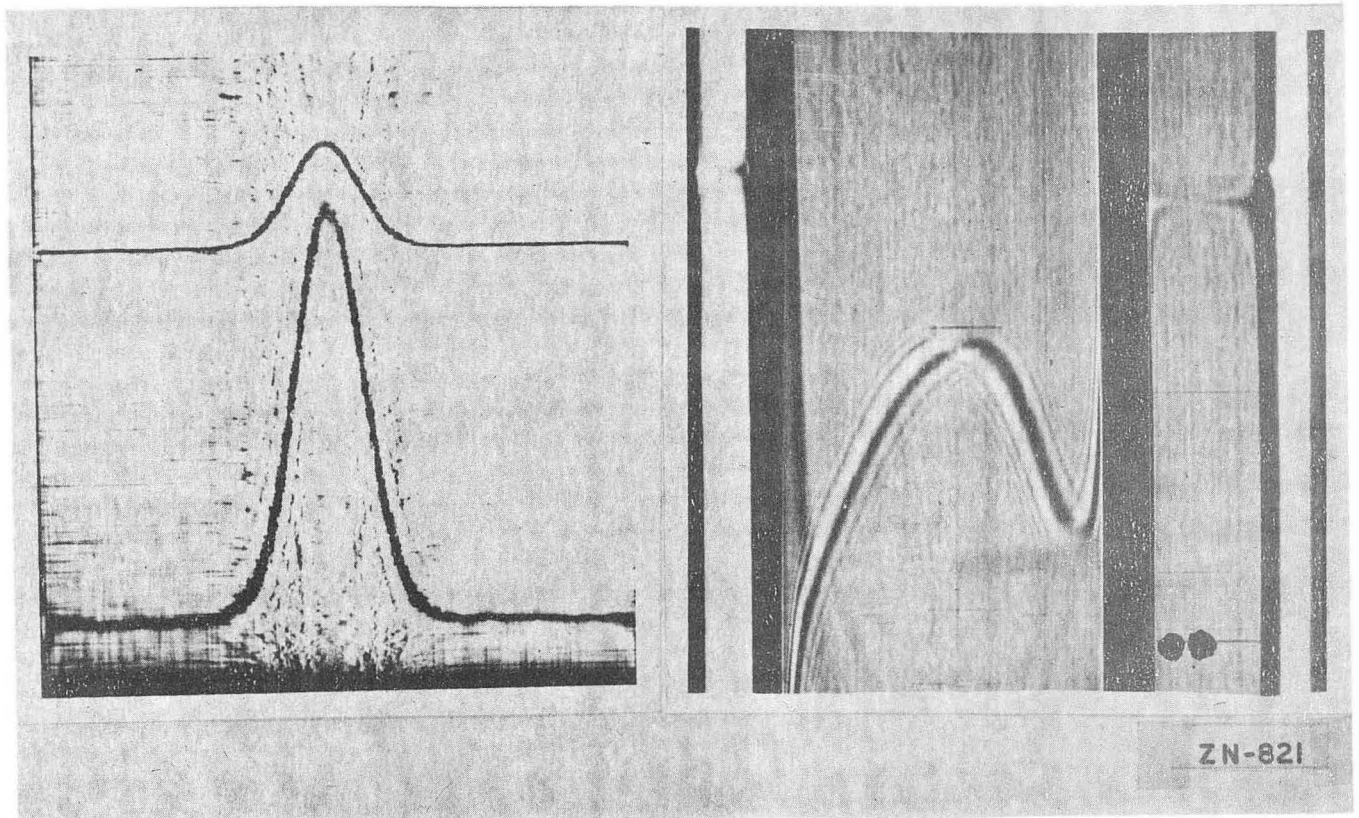


Fig. 2 - Special imperfect phaseplates

- (a) Unpolished plate glass
- (b) Rounded edge of phaseplate coating

In spite of the mottled background, the phaseplate in (a) gives legible patterns. The baseline regions have been made visible by attaching a fine wire (0.003" dia.) along the phaseplate edge.

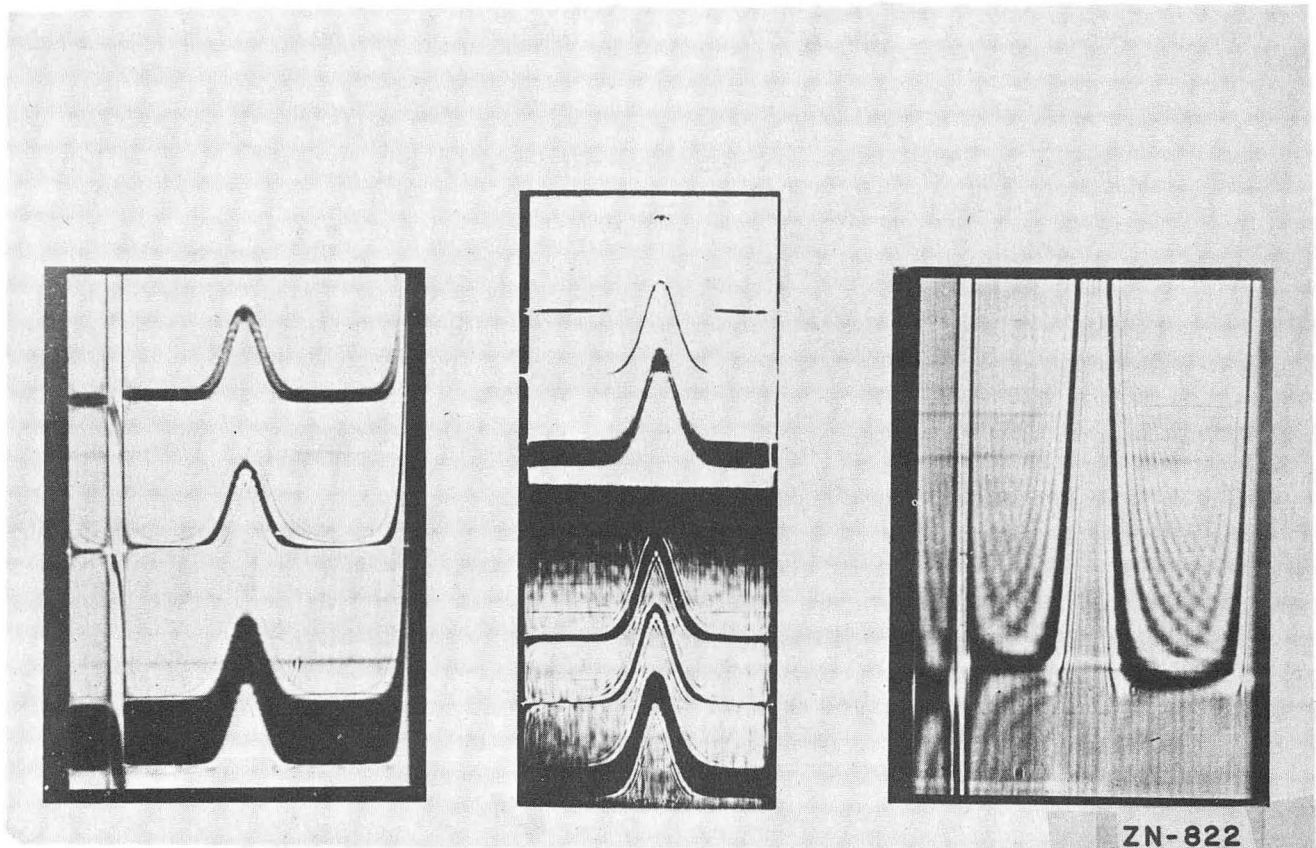


Fig. 3 - Comparison of bar, wire and phaseplate as schlieren diaphragms simultaneously

- (a) and (b) Upper pattern 0.010" wire  
Middle pattern phaseplate  
Lower pattern 1.5 mm bar
- (a) Ultracentrifuge. Synthetic boundary cell.  
Mineral oil on top of protein solution.
- (b) Electrophoresis. Two exposures shown  
Above: overexposure  
Below: normal exposure
- (c) High magnification ( $15^\circ$  diaphragm angle)  
of phaseplate pattern of (a).

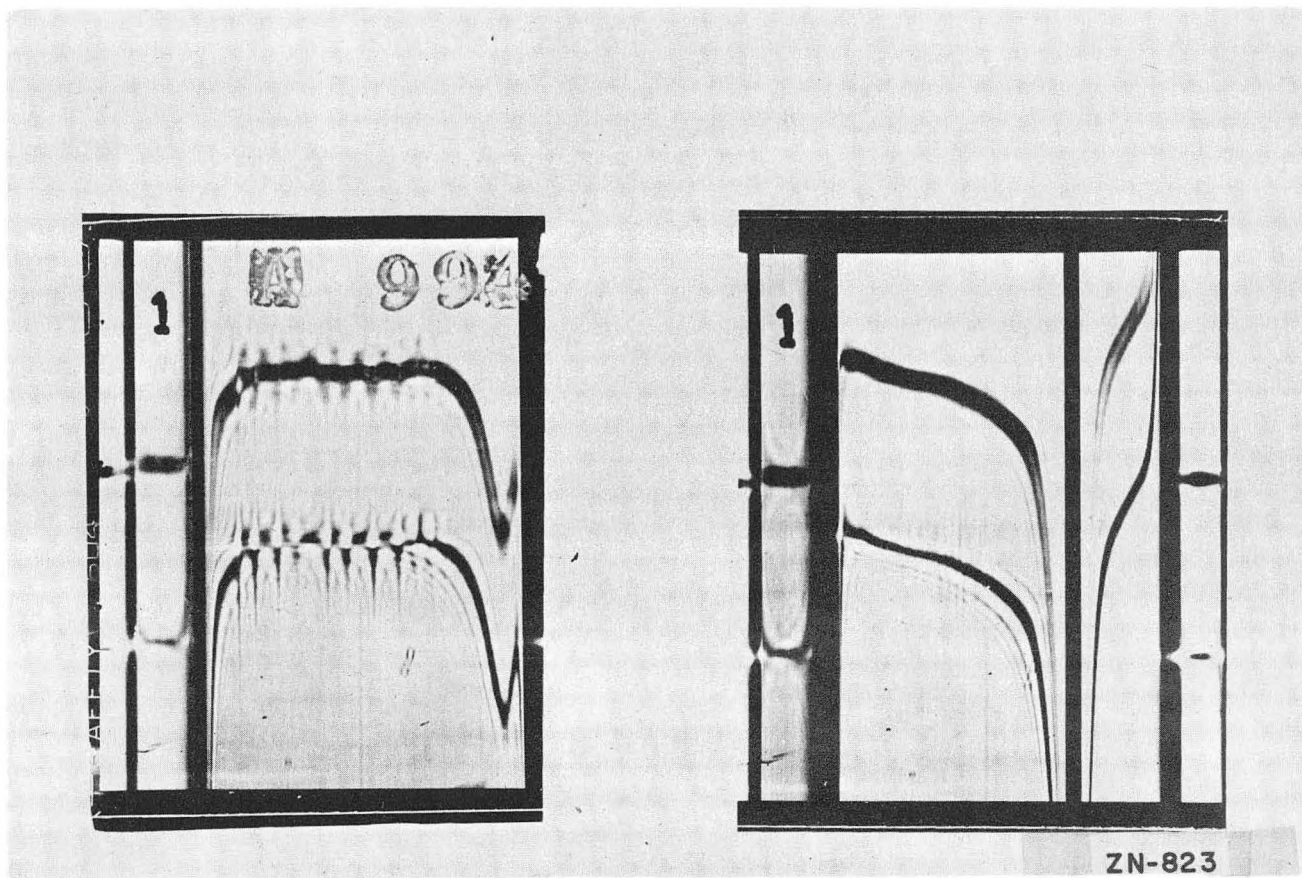


Fig. 4 - Comparison of wire and phaseplate in analytical ultracentrifugal flotation lipoprotein run.

(a) First frame 2' after attaining 52,640 RPM

(b) Sixth frame 38' after attaining 52,640 RPM

Single cell; upper pattern-wire; lower pattern-phaseplate

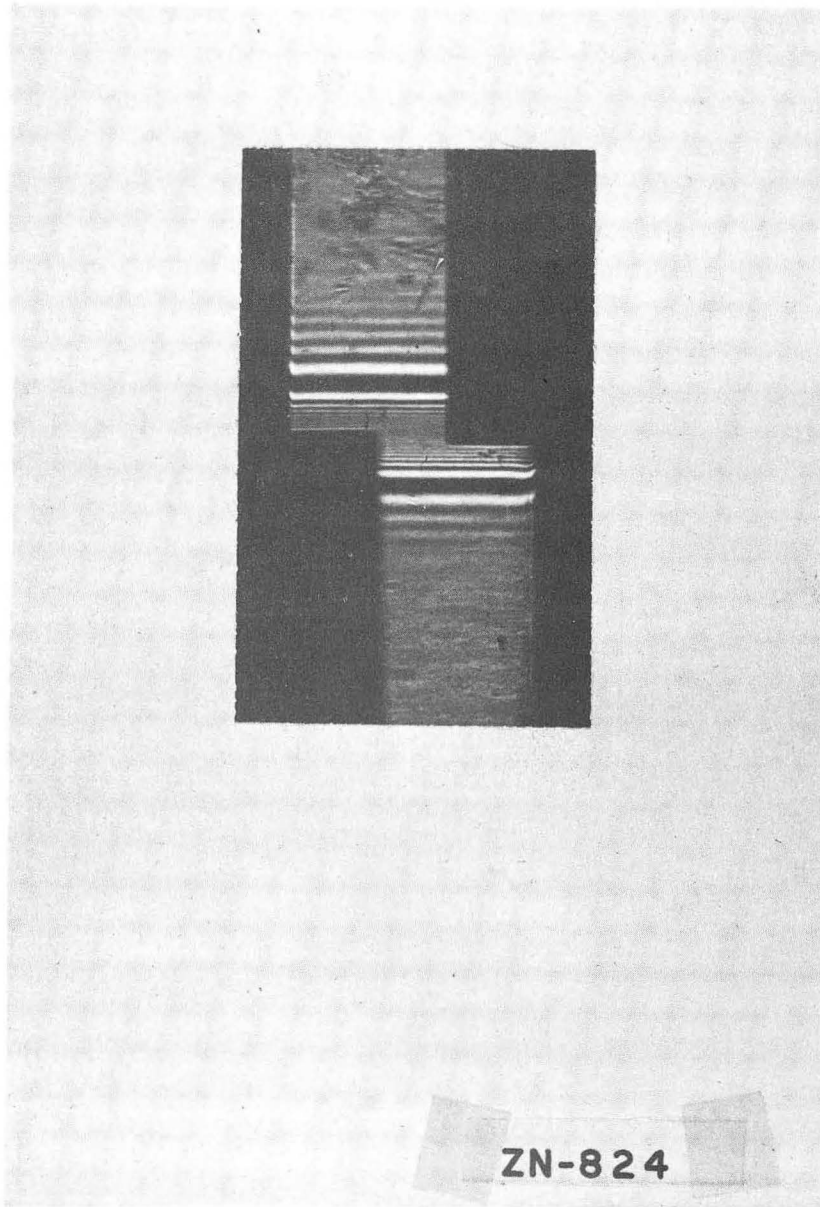


Fig. 5 - Anomalous diffraction effect

Selective masking of certain boundary regions showing independence of light rays of the same deflection in determining the Fresnel diffraction pattern which has closer spacing inside the boundary than outside.

Horizontal phaseplate in scanning schlieren camera. Solvent (upper) buffer, solution (lower), 0.3% protein. Left, masking out solution side of boundary maximum gradient, right, masking out of solvent side of boundary maximum gradient.

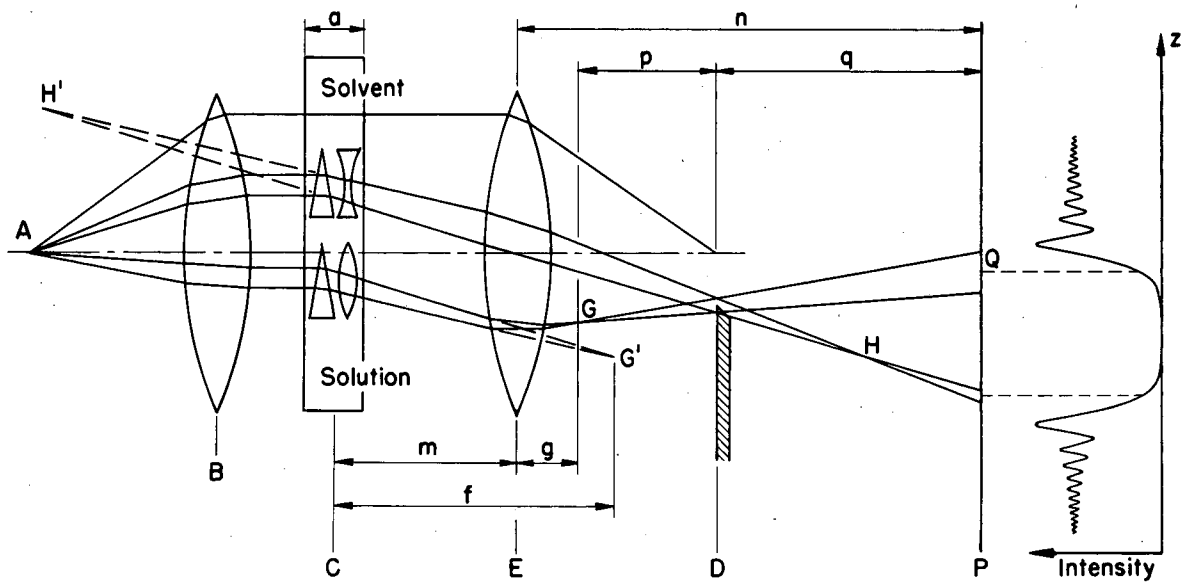


Fig. 6 - Schematic equivalent schlieren optical system

- A. Light source
- B. (First) schlieren lens
- C. Cell
- D. Schlieren diaphragm
- E. (Second) schlieren lens and camera objective
- G. Light-source image for rays passing through solution side of maximum refractive-index gradient
- H. Light-source image for rays passing through solvent side of maximum refractive-index gradient
- P. Photographic plate or ground glass

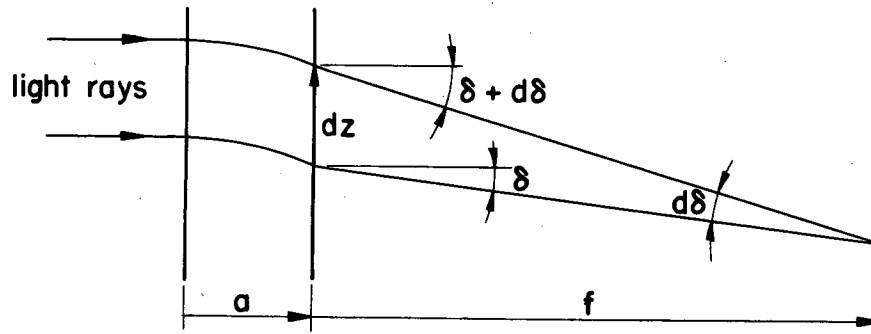


Fig. 7 - Lens action of a refractive index gradient

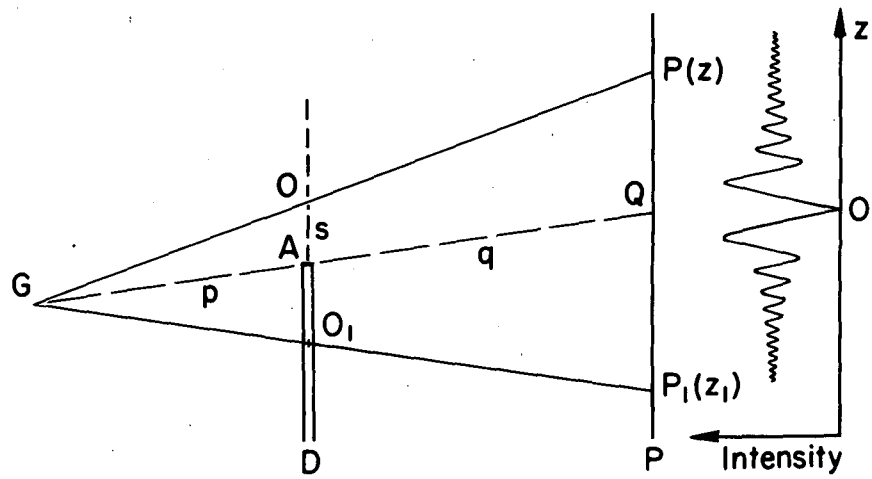


Fig. 8 - Fresnel diffraction from a phaseplate



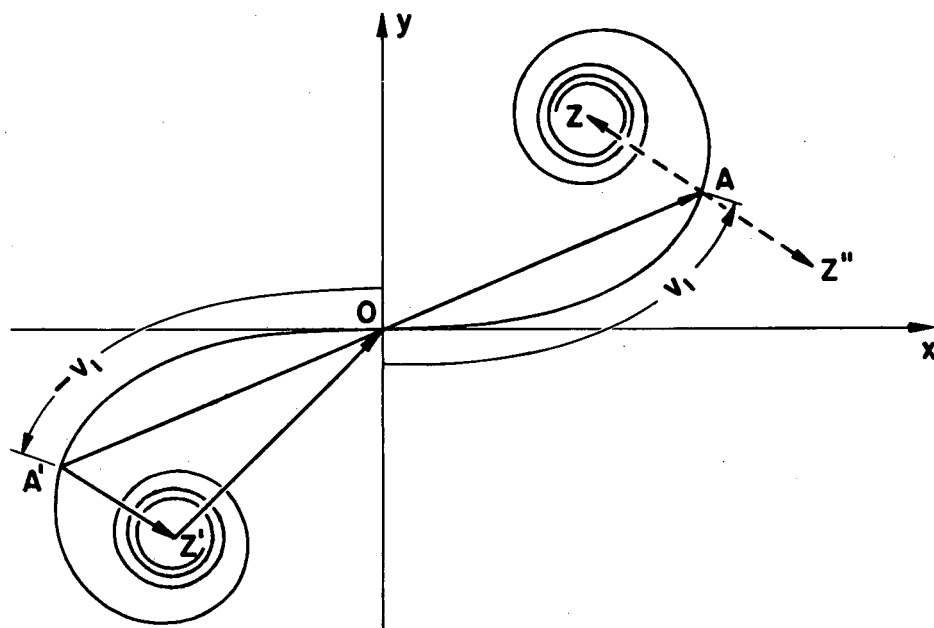


Fig. 9 - Cornu Spiral used in solution of the diffraction pattern from a phaseplate.